AD-A265 705

TATION PAGE

Form Approved
OMB No. 0704-0188

to average 1 hour per response, including the time for reviewing instructions, searching existing data sources
wing the collection of information. Send comments regarding this burden estimate or any other aspect of this
en, to Washington Headquarters Services, Directorate for Information Operations and Reports, 1215 Jefferson
e of Management and Budget, Paperwork Reduction Project (0704-0188), Washington, DC 20503

DATE
May 12, 1993

3. REPORT TYPE AND DATES COVERED
Technical Report /June 1992-May 1993

4. TITLE AND SUBTITLE
A Vibrational Spectroscopic Study of the Structure of Electroactive Self-Assembled Monolayers of Viologen Derivatives

5. FUNDING NUMBERS
Grant # N00014-90-J-1167
R&T Code 4133019

②

6. AUTHOR(S)
Xiaoyan Tang, Thomas Schneider, and Daniel A. Buttry

7. PERFORMING ORGANIZATION NAME(S) AND ADDRESS(ES)
Department of Chemistry, University of Wyoming
Laramie, WY 82071-3838

8. PERFORMING ORGANIZATION REPORT NUMBER

9. SPONSORING/MONITORING AGENCY NAME(S) AND ADDRESS(ES)
Office of Naval Research
Chemistry Division
800 N. Quincy Street
Arlington, VA

DTIC
ELECTE
JUN 14 1993
S A D

10. SPONSORING/MONITORING AGENCY REPORT NUMBER
Technical Report #20

11. SUPPLEMENTARY NOTES
Prepared for publication in Langmuir

12a. DISTRIBUTION/AVAILABILITY STATEMENT
This document has been approved for public release and sale; its distribution is unlimited

12b. DISTRIBUTION CODE

13. ABSTRACT *(Maximum 200 words)*

Surface Enhanced Raman and glancing angle FTIR are used to characterize the structure of self-assembled monolayers of viologen derivatives at electrode surfaces. Both techniques rely on the surface selection rules. These

monolayers were found to have some degree of order, with the long axis of the viologen group found to be along the surface normal.

93-13169

93 064

14. SUBJECT TERMS
surface-enhanced Raman, electrochemistry, FTIR

15. NUMBER OF PAGES
22

16. PRICE CODE

17. SECURITY CLASSIFICATION OF REPORT	**18. SECURITY CLASSIFICATION OF THIS PAGE**	**19. SECURITY CLASSIFICATION OF ABSTRACT**	**20. LIMITATION OF ABSTRACT**
unclassified	unclassified	unclassified	UL

OFFICE OF NAVAL RESEARCH

Grant # N00014-90-J-1167

R&T Code 4133019

Technical Report #20

A Vibrational Spectroscopic Study of the Structure of Electroactive Self-Assembled Monolayers of Viologen Derivatives

by

Xiaoyan Tang, Thomas Schneider, and Daniel A. Buttry

Prepared for Publication in

Langmuir

Department of Chemistry
University of Wyoming
Laramie, WY 82071-3838

May 12, 1993

A Vibrational Spectroscopic Study of the Structure of Electroactive Self-Assembled Monolayers of Viologen Derivatives

Xiaoyan Tang, Thomas Schneider and Daniel A. Buttry*
Department of Chemistry
University of Wyoming
Laramie, WY 82071-3838

Abstract - Surface enhanced Raman spectroscopy (SERS) and infrared reflection absorption spectroscopy (IRRAS) are used to determine the orientation of the viologen redox group and the relative degree of ordering of the alkyl chain segments in self-assembled monolayers of various alkyl viologen derivatives. The monolayers were assembled and examined on rough Ag electrodes (SERS) and smooth, vapor-deposited Au electrodes (IRRAS). Attachment to the Ag or Au surfaces which were studied occurs by virtue of strong interaction of a disulfide group on the molecule with the surface. In the present case, analysis of the relative intensities of the viologen A_g N-R stretching mode at 1169 cm^{-1} and two of the A_g ring modes at 1298 and 1637 cm^{-1} reveals that the net orientation of the long axis of the viologen moiety is roughly perpendicular to the plane of the electrode surface, in accordance with the surface coverages at saturation as determined from previous electrochemical data. The relative intensities of the methylene asymmetric (2890 cm^{-1}) and symmetric (2850 cm^{-1}) stretches in the SERS spectra on rough Ag and the peak positions of the asymmetric and symmetric methylene C-H stretching modes in the IRRAS on smooth Au (at 2929 cm^{-1} and 2857 cm^{-1}, respectively) reveal a liquid-like environment for the alkyl chains. These results are consistent with the relative sizes of the viologen and alkyl groups and the expected packing arrangement based on these, as well as with previous electrochemically derived surface coverages for saturated SAM's of these compounds.

Introduction

The spontaneous assembly of molecules at surfaces represents a simple and powerful method of constructing interfaces with well-defined structure and composition. Due to these characteristics, many groups are engaged in studies of self-assembled monolayers (SAM's) (1). A significant use of these assemblies is in understanding now interfacial structure influences chemistry and physics at the interface, with the long range goal of learning to control interfacial processes. Our group has also been using electroactive SAM's in an effort to understand how the interfacial environment affects interfacial redox processes. In particular, the influence of ion pairing (2,3) and the position of the redox group within the monolayer structure (4) have been shown to significantly impact the electrochemistry (especially the formal potential) of the redox moiety within the SAM. The finding that subtle details of the SAM structure and positioning of the redox group within it can have such major influence on electron transfer to the pendent or embedded redox group has prompted us to more closely examine the structural details of these systems. Thus, as a complement to our previous work on the electrochemistry of viologen SAM systems, we present here a vibrational spectroscopic study of the structure of the SAM's formed from these viologen derivatives.

Several other groups (5-9) also have investigated monolayers of amphiphilic viologens derivatives which spontaneously adsorb at electrode surfaces either in the V^{2+} state or in the one-electron reduced V^{+} state. However, the SAM's formed from the derivatives described here differ in that they bear disulfide linkages capable of forming covalent anchors to the Ag electrode surfaces used in the study. Thus, these monolayers are expected to have better structural regularity as well as less dynamic behavior than those without anchoring groups.

Experimental

The silver SERS electrode was constructed from flattened high purity silver wire which was sealed in a Teflon plug with Torr Seal. The silver electrode surface was polished mechanically using increasingly smaller sizes of alumina powder (to 0.05 μm) and washed ultrasonically in deionized water. It was then roughened in 0.1M NaCl by a double potential step using a conventional three-electrode cell and a PAR Model 273 potentiostat. A double potential step sequence of -0.2V to +0.2V or 0.25V and back to -0.2V versus SCE, with a dwell time of 2 to 4 seconds at +0.2V or 0.25V was usually used to roughen the surface. The dwell time was determined by the charge passed. It has been agreed that a charge range from

30 to 50 mC cm^{-2} gives maximum SERS intensity. The dimensions of the exposed, rectangular electrode surface were ca 1x10 mm. The Raman cell which was used to obtain SERS spectra was constructed in the shape of a cylinder with an optically flat window. A Ag/AgCl electrode served as a reference electrode (to which all potentials are referenced) and a platinum wire was used as the counter electrode. The roughened silver electrode was used as the working electrode. The electrolyte in the Raman cell was deaerated by purging with argon before the experiments. Careful attention to exclusion of air is required for these experiments due to the extreme sensitivity of the reduced forms of viologens to oxygen.

The optically smooth Au electrodes were prepared by vapor deposition in an Edwards 306A oil diffusion-pumped vacuum chamber. Float glass microscope slides were carefully cleaned with various acid treatments followed by rinsing with organic solvents and immediate placement into the vacuum chamber. 10 nm of Cr were deposited as an adhesion layer after which 250 nm of Au were deposited. These substrates were cleaned with 50/50 concentrated sulfuric acid and 30% H_2O_2 just prior to monolayer assembly.

The compounds are referred to in the following way: $CH_3(CH_2)_9V^{2+}(CH_2)_{10}SS(CH_2)_{10}V^{2+}(CH_2)_9CH_3$, where V^{2+} designates the viologen redox group, is referred to as $(10V10S\text{-})_2$, with the number referring to the number of carbons in the alkyl chain. Other compounds are referred to analogously. $(10V10S\text{-})_2$ was synthesized by the method described in reference 2. We note here that the synthetic route to these compounds described in reference 2 actually produces a disulfide, rather than a thiol, derivative. We will discuss this in a future contribution along with a description of the differences in behavior of these two self-assembling systems. Monolayers of all compounds were formed by immersing the roughened Ag electrode or the smooth Au surface into a dilute (typically 0.1 mM) aqueous electrolyte solution of the compound of interest for a time period ranging from several hours to days. In case the compound was not reasonably soluble in water up to 50% of ethanol was used to improve solubility. Obtaining normal Raman spectra of these viologen derivatives required highly purified material due to the presence of traces of fluorescent impurities following the synthetic route which was employed. Purification was accomplished by repeated recrystallizations, typically at least five times.

In-situ Raman spectra were obtained using a 90 degree excitation/collection geometry. Spectra were taken with a SPEX 1700 series single pass monochromator, a RCA C31034 PMT detector which was cooled by dry ice, and Ortec photon counting electronics.

Raman spectra were collected and stored with an IBM personal computer interfaced to the monochromator. A 43068 interference filter (Edmund Scientific) and a Holographic Long Pass 1005 filter (Kaiser Electrooptics) were used to remove plasma lines and to reduce the intensity of Rayleigh scattering, respectively. An f/1.8 collection lens was used to collect and focus the Raman scattered light through the monochromator. A Lexel Model 94 argon ion laser provided 514.5 nm excitation. Spectral resolution was typically 5 cm^{-1} and integration times were typically 1-10 seconds per point.

Ex-situ IRRAS spectra were obtained with a Bomem MB100 FTIR using a HgCdTe liquid nitrogen-cooled detector and a Harrick VRA glancing angle attachment set at 80°. Backgrounds were obtained using a perdeuterated hexadecane thiol monolayer so as to avoid any hydrocarbon interference in the background. Spectra were obtained at 4 cm^{-1} resolution with 512 scans.

Results

A. SAM and Model Compound IR and Raman Spectra

As discussed previously, these viologen systems self-assemble on Au electrodes to form stable monolayers which exhibit the well-defined electrochemistry of the viologen group (2,4). Similar behavior is shown in Figure 1 for a SAM on a rough Ag electrode. The two, reversible, one-electron redox processes of the viologen redox group are clearly observed. The potentials of the first and second redox processes (ca. -0.45 and -0.90 V, respectively) correlate well with those previously observed for SAM's of this same molecule on Au electrodes (2,4). The response of a typical SAM on a Ag electrode is stable for several hours, indicating virtually irreversible adsorption of these disulfide derivatives onto the Ag electrode.

Figure 2A shows the normal Raman spectrum of a highly purified viologen derivative (N,N'-dimethyl-4,4'-bipyridinium sulfate, $MVSO_4$), and Figure 2B shows the SERS spectrum of a $(10V10S-)_2$ SAM on a rough Ag electrode in the 900-1700 cm^{-1} region. A salient feature of these spectra is the difference in the integrated intensity ratios of the bands at 1169 cm^{-1}, 1298 cm^{-1}, and 1637 cm^{-1} for these two samples. These bands correspond to the viologen A_g N-R stretching mode for the bond between the pyridinium nitrogen and the pendent alkyl chain (1169 cm^{-1} for the SAM, 1187 cm^{-1} for $MVSO_4$) and A_g ring modes (1298 and 1637 cm^{-1} for the SAM, 1289 and 1646 cm^{-1} for $MVSO_4$). We return to a discussion of these assignments and relative intensities below.

Figure 3A shows the C-H stretching region of the SERS spectrum of the $(10V10S\text{-})_2$ SAM on rough silver. This spectrum shows a strong band for the aromatic C-H stretching modes near 3080 cm^{-1}, as well as the methylene and methyl C-H stretching envelope between 2820 and 3000 cm^{-1}. Figure 3B shows the same region for liquid octane thiol. The ratio (I_{2890}/I_{2850}) of the peak heights of the methylene asymmetric (2890 cm^{-1}) and symmetric (2850 cm^{-1}) C-H stretching modes, which has been used to reveal the degree of "order" in polymethylene systems (10,11), is seen to be quite similar for these two samples. This strongly suggests that the alkyl chains in these monolayers are in a liquid-like environment.

Figure 4 shows an ex-situ IRRAS glancing angle spectrum in the C-H stretching region of a $(10V10S\text{-})_2$ SAM on a smooth Au surface. The peak intensities of the methylene C-H stretching modes are consistent with formation of a single monolayer of material in these SAM's (12-14). Previous workers have used the peak positions of the asymmetric and symmetric methylene C-H stretches to reveal the degree of ordering of the alkyl chains in thiol-anchored SAM's of alkane thiols (12) and ferrocene terminated, electroactive SAM's (13,14). In the present case, these peak positions (asymmetric at 2929 cm^{-1} and symmetric at 2857 cm^{-1}) are consistent with a liquid-like environment for the alkyl chains, in agreement with the SERS results.

Figure 5 shows the normal FTIR spectrum of a bulk sample of the dibromide salt of $(10V10S\text{-})_2$ (curve 1) and the IRRAS glancing angle spectrum of a $(10V10S\text{-})_2$ SAM in the 1000-1800 cm^{-1} region. This spectrum is of the same SAM as that shown in Figure 4 above. Note that while the ring mode at 1637 cm^{-1} is the most pronounced peak in this region of the spectrum for the dibromide salt of $(10V10S\text{-})_2$, this band is virtually absent from the IRRAS spectrum.

B. Characterization of the Rough Ag Surfaces

Given the observations of liquid-like alkane chains in the viologen SAM's described above, we undertook a set of experiments designed to characterize the extent to which these SERS-active, rough Ag surfaces could support formation of reasonably well-ordered SAM's. The question is whether the liquid-like nature of the viologen SAM's is due to the surface roughness of the Ag SERS substrates or the intrinsic ability of these molecules to pack efficiently. Assembly of SAM's of alkyl thiols was choosen as a good test of this tendency.

Figure 6 shows the SERS spectrum of a SAM formed from octane thiol on a Ag electrode roughened in the same way as those used for the viologen SAM studies described above. Comparison of the ratio (I_{2890}/I_{2850}) of the peak heights of the methylene asymmetric (2890 cm^{-1}) and symmetric (2850 cm^{-1}) C-H stretching modes for the SAM ($I_{2890}/I_{2850} = 1.2$) with that of liquid octane thiol in Figure 3b above ($I_{2890}/I_{2850} = 0.85$) indicates substantially more order in the octane thiol SAM than in the liquid.

Another measure of the degree of order within a SAM can be obtained by examination of the Raman spectral region which contains the C-S stretching modes. Two distinct bands are seen for the C-S stretches which correspond to gauche (635 cm^{-1}) and trans (705 cm^{-1}) conformations around the two carbon atoms adjacent to the S atom. This region has been used by Joo and coworkers (15) and Pemberton and coworkers (16) to estimate the relative amounts of gauche and trans conformers in SAM's. They showed that highly ordered SAM's and solid alkyl thiols show large proportions of the trans conformer compared to the gauche conformer, in accordance with expectations.

Figure 7A shows the SERS spectrum of an octane thiol SAM on a rough Ag surface, and Figure 7B shows a normal Raman spectrum of liquid octane thiol. The liquid spectrum clearly shows both trans (ca. 730 cm^{-1}) and gauche (ca. 650 cm^{-1}) conformers to be present in the octane thiol liquid sample. On the other hand, the SERS spectrum of the octane thiol SAM shows a very strong band at 700 cm^{-1} and only a very small band at 620 cm^{-1}. These bands are attributed to the trans and gauche conformers, respectively. The large energy shifts of these bands have been suggested to be due to strong interaction with the Ag surface atoms (16). The predominance of the trans band strongly suggests that it is possible to form modestly well-ordered SAM's on the rough Ag surface. The relative intensities of the trans and gauche bands (ca. 20:1) suggests a defect density of 1-5%.

Another test of the extent to which formation of reasonably well-ordered SAM's can occur on these rough Ag surfaces is based on relative permeability of the SAM toward solution phase redox couples. To address this question the currents for methyl viologen reduction at a rough, bare Ag and at a rough, SAM covered Ag surface were examined. A very crude measure of the defect density in the monolayer can be obtained from the ratio of the plateau current at the (microelectrode-like) SAM surface (17) to the peak current at a rough, bare Ag surface. This ratio is ca. 0.01, consistent with a SAM which contains some defects (pinholes, etc.), but is not so lacking in structural integrity as to allow unrestricted access of solution phase species to the underlying Ag electrode.

Discussion

The vibrational spectroscopic properties of viologens and their reduction products, especially the symmetrically substituted N,N'-dimethylviologen (MV^{2+}), have been frequently studied. The first paper concerning the Raman spectra of methylviologen was published by Benchenane et al. in 1974 (18). Since then many papers on the Raman and infrared spectra of viologens, mainly methylviologen, have been published. Among them the works of Cotton and her co-workers (2,19-24), Hester and his co-workers (25-27) and Poizat and his co-workers (28-32) are very representative. The first normal coordinate analysis of the in-plane vibrational modes of MV^{2+} and its reduction product, the cation radical MV^{+}, was made in 1982 (26). This was then extended to the three redox forms of methylviologen in 1988 (21). These normal mode calculations combined with all the experimental data available (including isotopic substitutions) have made it possible to reach a general agreement on assignment of most bands of the three redox forms of methylviologen. These assignments are used as the basis of the discussion below.

The ready availability of strong Raman bands which have polarizability changes perpendicular to each other allows use of the surface selection rule (35-38) to estimate the orientation of the viologen ring system with respect to the surface normal. Briefly, because of the relative enhancement (via surface plasmon excitation at the rough surface) of the component of the optical field which is perpendicular to the surface over that which is parallel to the surface, those modes which produce polarizability changes perpendicular to the surface are enhanced relative to those which produce polarizability changes parallel to the surface. In favorable cases, it is possible to use this effect to quantitativety calculate molecular orientations (39). In the present case, the fact that these bands contain contributions from more than one mode (see below) precludes a detailed, quantitative orientational analysis. However, it is possible to make qualitative statements about relative orientation, as has been done in the past in analyses of this type on monolayer and multilayer deposits of viologens at electrodes (2,19-24).

For purposes of discussion, it is useful to impose a coordinate axis on the viologen molecule. Figure 8 shows the structure of a generalized viologen derivative, along with an arbitrarily chosen axis system. The symmetry is taken to be D_{2h}, implying a coplanar arrangement of the two rings, consistent with previous vibrational spectroscopic studies (2,18-32) and x-ray crystal structures (33,34). From the body of work described above, there is general agreement that the band at 1169 cm^{-1} is mainly derived from the A_g N-R stretch between the ring nitrogen and the first methylene group in the chain. Thus, the predominant component of the polarizability change for this mode is along the x-axis of the coordinate system (the long axis of the molecule). The 1298 and 1637 cm^{-1} bands are A_g ring modes which are mainly derived from C-C and C-N stretches for atoms within the ring system. It has been previously argued that, since the N-R stretch has its polarizability change directly along the x-axis, it should be more enhanced than either the 1298 or 1637 cm^{-1} ring modes by virtue of the surface selection rules (2). This argument has generally been consistent with experimental results from other sources (e.g. electrochemical studies) and appears to be valid.

One manner of examining the enhancement due to orientation of the viologen group is to compare the ratio of the integrated intensities of the 1169 and 1298 cm^{-1} bands (i.e. I_{1169}/I_{1298}) for an isotropic (i.e. unoriented) bulk sample and for a SAM. In the present case these ratios are 0.5 for the $MVSO_4$ sample and 1.3 for the SAM. Thus, the integrated intensity ratio for the SAM is enhanced by a factor of 2.6 relative to that for the bulk $MVSO_4$ sample. This implies a high degree of orientation of the long axis of the viologen group along the surface normal in these SAM's.

The IRRAS data given in Figure 5 also provide convincing evidence of the degree of orientation of the viologen group in the SAM. These data show that, while the 1637 cm^{-1} band is the most intense band in the 1000-1800 cm^{-1} region of the FTIR spectrum of the bulk sample, it is barely visible in the SAM IRRAS spectrum. This band has been assigned as due to a B_{2u} ring mode by both Cotton and coworkers (21) and Hester and coworkers (26). This assignment defines the dipole moment change as along the y-axis for the coordinate system shown in Figure 8. Thus, the observation of a very weak absorption for this mode suggests that the y-axis of the molecule is parallel to the Au surface. This could be achieved either with flat-on or perpendicular orientation of the ring system (or any angle between). However, this result precludes edge-on orientations.

Taken together, the SERS and IRRAS data suggest that the viologen group is roughly perpendicular to the electrode surface. This is in accordance with expectations based on the saturation coverage of this molecule on smooth Au surfaces, which has been previously found to be (3.5-3.9) x 10^{-10} mol cm^{-2} (2,4). Other studies on similar self-assembling viologens with long alkyl chains which are not functionalized with groups capable of anchoring the molecule to the surface (5-9), as well as Langmuir-Blodgett (LB) monolayers of long chain viologen derivatives (5,40,41) have reported similar coverages ((2-4) x 10^{-10} mol cm^{-2}). With the exception of one LB monolayer study (5) which gave surface coverages which were consistently lower (ca. 2 x 10^{-10} mol cm^{-2}) than those for the other systems (ca. 3-4 x 10^{-10} mol cm^{-2}), these findings all support a structure for saturated monolayers of viologen species bearing long alkyl chains in which the ring system is roughly perpendicular to the electrode surface.

The SERS and IRRAS spectra also offer information on the relative degree of order within the alkyl chain regions of the viologen SAM's. In particular, the ratio (I_{2890}/I_{2850}) of the peak heights of the methylene asymmetric (2890 cm^{-1}) and symmetric (2850 cm^{-1}) C-H stretching modes which has been used to reveal the degree of "order" in polymethylene systems has proven useful in the present case. Snyder and coworkers (10) have discussed the physical meaning of this peak height ratio in considerable detail. They point out that this ratio responds to both environment (i.e. lateral packing) and to conformational order, and that it is inappropriate to use this ratio under conditions of appreciable conformational disorder. Nevertheless, the similar values of this ratio and the very similar appearances of the C-H stretching envelope for the liquid octane thiol and viologen SAM would seem to imply that the alkyl chains are highly disordered, in a liquid-like environment. In addition, the IRRAS results suggest a liquid-like environment for the alkyl chains, based on the positions of the symmetric and asymmetric methylene C-H stretches.

The lack of a highly ordered alkyl chain region in these viologen SAM's seems reasonable given the fact that the projected area of the viologen group of these molecules (ca. 35-50 Å^2/molecule, depending on whether or not the counterions are included) is about twice that of the alkyl chains (ca. 18-20 Å^2/molecule). The difference is projected area of these moieties is readily apparent in the difference in the saturation coverage for the viologen SAM (ca. 4 x 10^{-10} mol cm^{-2} (2)) and for a n-alkyl thiol SAM (ca. 8 x 10^{-10} mol cm^{-2} (42). The fact that the larger viologen determines the packing density (because of the size disparity) is likely to be a significant impediment to efficient packing of the alkyl chains. This failure to achieve closest-packing of the alkyl chains is undoubtedly the cause of the spectral signatures for highly disordered alkyl chains which were observed. The results described above for the C-S stretching region of octane thiol SAM's on rough Ag make it clear that the surface roughness of the Ag SERS substrates is not the cause of the poor degree of order of the alkyl chains in the viologen SAM's.

The data reported here for these viologen derivative SAM's and those previously reported by others for the alkyl viologen SAM's and LB monolayers can also be compared to two studies by Ulman and coworkers (43,44) of monolayers formed from n-alkyl chains with polar aromatic groups embedded within the chain and having either a trichlorosilane or thiol group for SAM formation on Si or Au surfaces, respectively. Specifically, they studied assembly on Au (44) of molecules with either a para-oxyphenyl sulfone or p-oxyphenyl sulfide group embedded within the alkyl chain (i.e. $CH_3(CH_2)_{m-1}SO_2(C_6H_6)O(CH_2)_nSH$ or $CH_3(CH_2)_{m-1}S(C_6H_6)O(CH_2)_nSH$, with the following m,n combinations; 12,4; 8,8; 4,12; 11,5), and assembly on Si (43) of a p-oxyphenyl sulfone derivative (i.e. $CH_3(CH_2)_{11}SO_2(C_6H_6)O(CH_2)_{11}SiCl_3$). They used a wide variety of methods to characterize these SAM's, including contact angle measurements, FTIR, ellipsometry, surface potential measurements, XPS, and SERS. The conclusions of these two complementary studies were that these molecules form relatively high quality SAM's which generally exhibit spectroscopic and wetting behavior similar to SAM's formed from the simpler n-alkyl thiols on Au. In particular, the FTIR data were consistent with an increasingly more ordered environment for the alkyl chains as the length of the alkyl chain above the buried polar group was increased. However, the data also revealed that the SAM's with buried polar groups are not, in general, as highly ordered as the n-alkyl thiol SAM's. Their findings are consistent with the conclusions of the present and previous studies regarding the structure of the viologen SAM's, namely, that the ring system is reasonably well-oriented, and predominantly perpendicular to the surface at saturation coverage. A caveat is that the slightly larger size of the viologen ring system (including its associated counterions) compared to the polar ring systems they studied precludes efficient packing of the alkyl chains and adoption of the all-trans conformation.

Conclusions

The picture which emerges from the present work is one in which the SAM's formed at saturation coverage from these viologen derivatives place the long axis of the viologen ring systems roughly perpendicular to the electrode surface, and have alkyl chain regions which are liquid-like. This ability to impose orientation on the buried group implies that it should be possible for these and other systems with embedded groups to control (and also systematically vary) a variety of structural parameters of the SAM, including the distance of the redox group from the electrode surface or the monolayer/solution interface, and the degree of exposure of the redox group to the solution phase environment. Control of this sort allows for the fabrication of experimental systems designed to probe the distance dependence of various phenomena, such as electron transfer rates (45,46) and the interfacial electric field strength (47). It might also allow one to manipulate the optical properties of monolayer or multilayer films by manipulating the distances between the chromophores and the underlying surface and between the chromophore layers, a degree of control which may prove essential to any potential non-linear optical applications based on SAM technology.

Acknowledgements

We are grateful to the Office of Naval Research for the full support of this work. We acknowledge Professor Carron for helpful discussions and a preprint.

References

1. Ulman, A. An Introduction to Ultrathin Organic Films: from Langmuir-Blodgett to Self-Assembly; Academic Press: Boston, 1991.
2. De Long, H. C.; Buttry, D. A. *Langmuir* **1990**, **6**, 1319-22.
3. De Long, H. C.; Donohue, J. J.; Buttry. D. A. *Langmuir* **1991**, **7**, 2196-202.
4. De Long, H. C.; Buttry, D. A. *Langmuir* **1992**, **8**, 2491-6.
5. Cotton, T. M.; Kim, J.-H.; Uphaus, R.A. *Microchem. J.* **1990**, **42**, 44-71.
6. Gomez, M.; Li, J.; Kaifer, A. E. *Langmuir* **1991**, **7**, 1797-806.
7. Diaz, A.; Kaifer, A. E. *J. Electroanal. Chem.* **1988**, **249**, 333-8.
8. Widrig, C. A.; Majda, M. *Langmuir* **1989**, **5**, 689-95.
9. Bae, I. T.; Huang, H.; Yeager, E. B.; Scherson, ~. A. *Langmuir* **1991**, **7**, 1558-62.
10. Snyder, R. G.; Hsu, S. L.; Krimm, S. *Spectrochim. Acta* **1978**, **34A**, 395-406.
11. Gaber, B. P.; Peticolas, W. L *Biochim. Biophys. Acta* **1977**, **465**, 260-74.
12. Porter, M. D.; Bright, T. B.; Allara, D. L.; Chidsey, C. E. D. *J. Am. Chem. Soc.* **1987**, **109**, 3559-68.
13. Walczak, M. M.; Popenoe, D. D.; Deinhammer, R. S.; Lamp, B. D.; Chung, C.; Porter, M. D. *Langmuir* **1991**, **7**, 2687-93.
14. Popenoe, D. D.; Deinhammer, R. S.; Porter, M. D. *Langmuir* **1992**, **8**, 2521-30.
15. Joo, T. H.; Kim, K.; Kim, M. S. *J. Phys. Chem.* **1986**, **90**, 5816-9.
16. Bryant, M. A.; Pemberton, J. E. *J. Am. Chem. Soc.* **1991**, **113**, 3629-37.
17. Sabatani, E.; Rubinstein, I. *J. Phys. Chem.* **1987**, **91**, 6663-9.
18. Benchenane, A.; Bernard, L.; Theophanides, T. *J. Raman Spectrosc.* **1974**, **2**, 543-53.
19. Kim, Jae-Ho; Cotton, T. M.; Uphaus, R. A. *J. Phys. Chem.* **1989**, **93**, 3713-20.
20. Feng, Q.; Yue, W.; Cotton, T. M. *J. Phys. Chem.* **1990**, 94, 2082-91.
21. Ghoshal, S.; Lu, T.; Feng, Q.; Cotton, T. M. *Spectrochim. Acta* **1988**, **44A**, 651-60.
22. Lu, T.; Cotton, T. M.; Hurst, J. K.; Thompson, D. H. P. *J. Phys. Chem.* **1988**, **92**, 6978-85.
23. Lu, T.; Cotton, T. M. *J. Phys. Chem.* **1987**, **91**, 5978-85.
24. Feng, Q.; Cotton, T. M. *J. Phys. Chem.* **1986**, **90**, 983-7.
25. Forster, M.; Girling, R. B.; Hester, R. E. *J. Raman Spectrosc.* **1982**, **12**, 36-48.
26. Hester, R. E.; Suzuki, S. J. Phys. Chem. **1982**, **86**, 4626-30.
27. Metcalfe, K.; Hester, R. E. *J. Chem. Soc., Chem. Commun.* **1983**, 133-5.
28. Poizat, O.; Giannotti, C.; Sourisseau, C. *J. Chem. Soc. Perkin Trans. II* **1987**, 829-34.
29. Poizat, O.; Sourisseau, C.; Corset, J. *J. Molec. Struc.* **1986**, **143**, 203-6.
30. Poizat, O.; Sourisseau, C.; Giannotti, C. *Chem. Phys. Lett.* **1985**, **122**, 129-32.

31. Poizat, O.; Sourisseau, C.; Mathey, Y. *J. Chem. Soc. Faraday Trans. I* **1984**, **80**, 3257-74.
32. Regis, A.; Corset, J. *J. chim. phys.* **1981**, **78**, 687-93.
33. Russell, J. H.; Wallwork, S. C. *Acta Cryst.* **1972**, **B28**, 1527-33.
34. Prout, C. K.; Murray-Rust, P. *J. Chem. Soc. (A)* **1969**, 1520-5.
35. Moskovits, M.; Suh, J. S. *J. Phys. Chem.* **1984**, **88**, 5526-30.
36. Moskovits, M. *Rev. Mod. Phys.* **1985**, **57**, 783-826.
37. Creighton, J. A. *Surf. Sci.* **1983**, **124**, 209-19.
38. ibid, **1985**, **158**, 211-21.
39. Jiang, Y.; Carron, K. to be submitted to J. Chem. Phys..
40. Lee, C.-W.; Bard, A. J. *Chem. Phys. Lett.* **1990**, **170**, 57-60.
41. Lee, C.-W.; Bard, A. *J. J. Electroanal. Chem.* **1988**, **239**, 441-6.
42. Widrig, C. A.; Chung, C.; Porter, M. D. *J. Electroanal. Chem.* **1991**, **310**, 335-59.
43. Tillman, N.; Ulman, A.; Elman, J. F. *Langmiur* **1990**, **6**, 1512-8.
44. Evans, S. D.; Urankar, E.; Ulman, A.; Ferris, N. *J. Am. Chem. Soc.* **1991**, **113**, 4121-31.
45. Chidsey, C. E. D. *Science* **1991**, **251**, 919-22.
46. Finklea, H. O.; Hanshew, D. D. *J. Am. Chem. Soc.* **1992**, **114**, 3173-81.
47. Pope, J. M.; Tan, Z.; Kimbrell, S.; Buttry, D. A. *J. Am. Chem. Soc.* **1992**, **114**, 10085-6.

Figure Captions

1. Voltammogram of a (1V12S-$)_2$ SAM on Ag in 0.1 M $NaNO_3$ with a scan rate of 100 mV s^{-1}, referenced versus SSCE.

2. Raman spectra in the ring mode region of (A) N,N'-dimethyl-4,4'-bipyridinium sulfate ($MVSO_4$) and (B) a (10V10S-$)_2$ SAM on a roughened Ag electrode at -0.1 V vs Ag/AgCl in 0.1 M phosphate buffer (pH=7.0).

3. Raman spectra in the C-H stretching region of (A) a (10V10S-$)_2$ SAM on a roughened Ag electrode at -0.1 V vs Ag/AgCl in 0.1 M phosphate buffer (pH=7.0) and (B) liquid octane thiol.

4. The infrared spectrum in the C-H stretching region of a (10V10S-$)_2$ SAM on a smooth Au surface.

5. Infrared spectra in the 1000-1800 cm^{-1} region of (1) the dibromide salt of (10V10S-$)_2$ in KBr and (2) a (10V10S-$)_2$ SAM on smooth Au.

6. The SERS spectrum in the C-H stretching region of an octane thiol SAM on a roughened Ag surface.

7. Raman spectra in the C-S stretching region of (A) an octane thiol SAM on a roughened Ag surface and (B) liquid octane thiol.

8. Molecular axes of a viologen derivative used in this work.

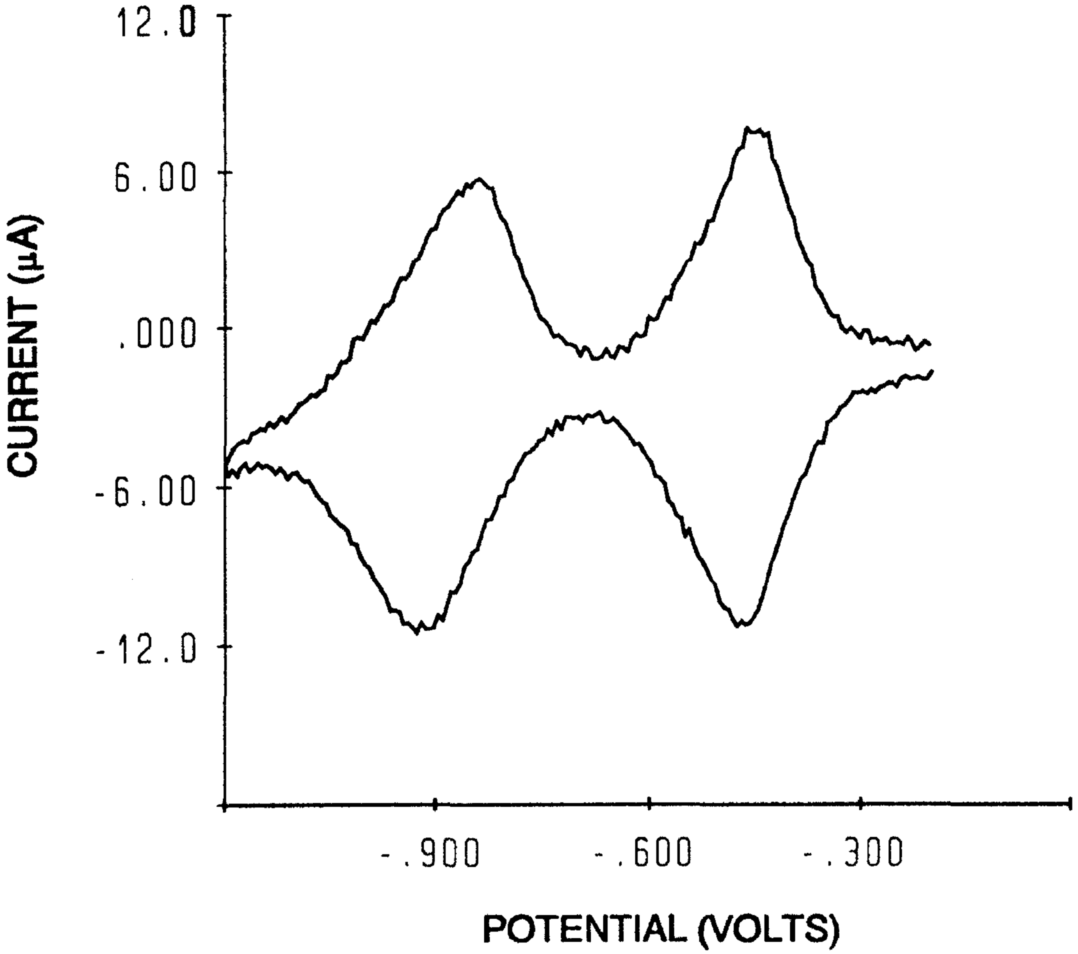
12.0
6.00
.000
-6.00
-12.0
CURRENT (μA)
-.900
-.600
-.300
POTENTIAL (VOLTS)

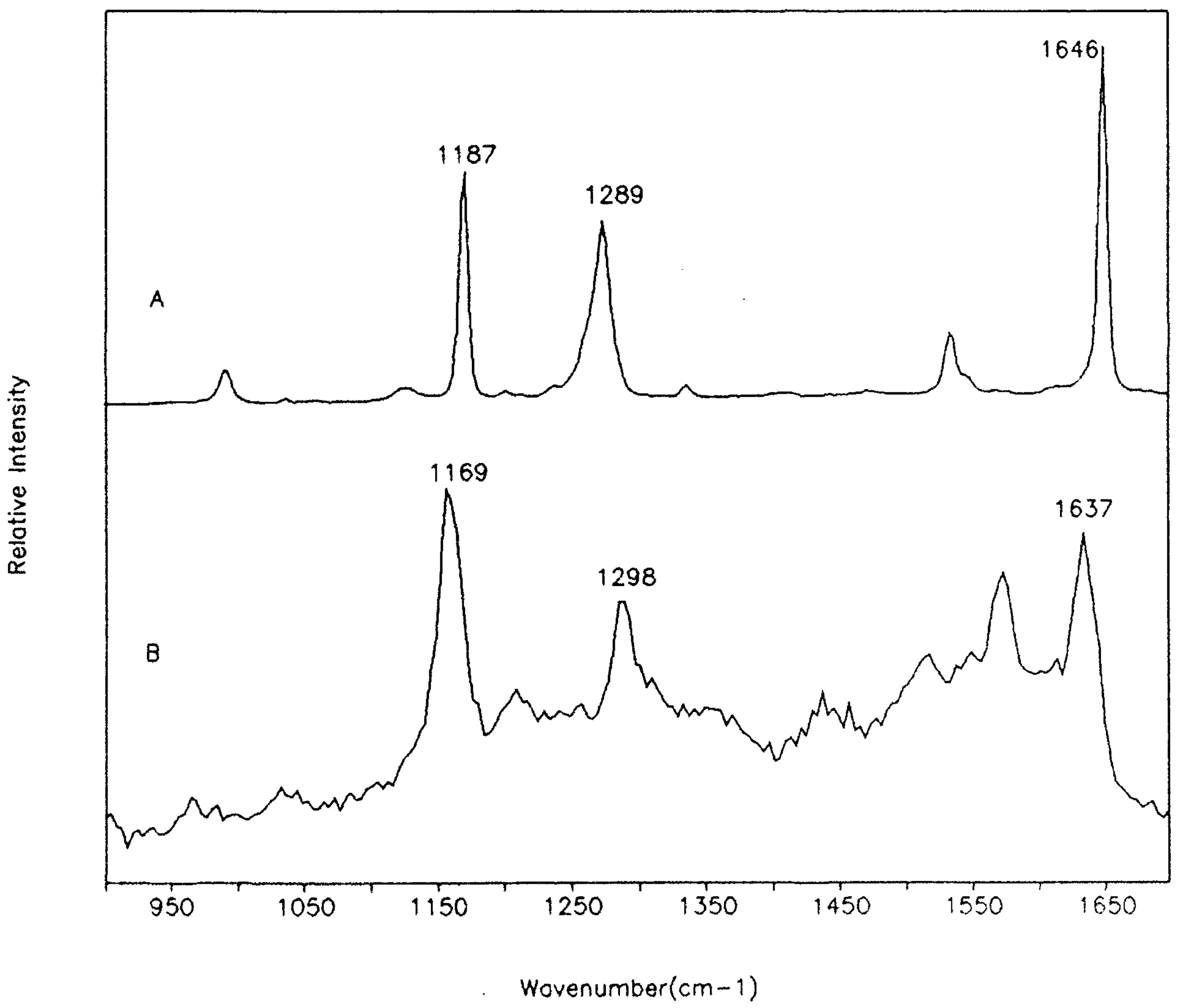
1646
1187
1289
A
1169
1637
1298
B
Relative Intensity
950
1050
1150
1250
1350
1450
1550
1650
Wavenumber(cm−1)

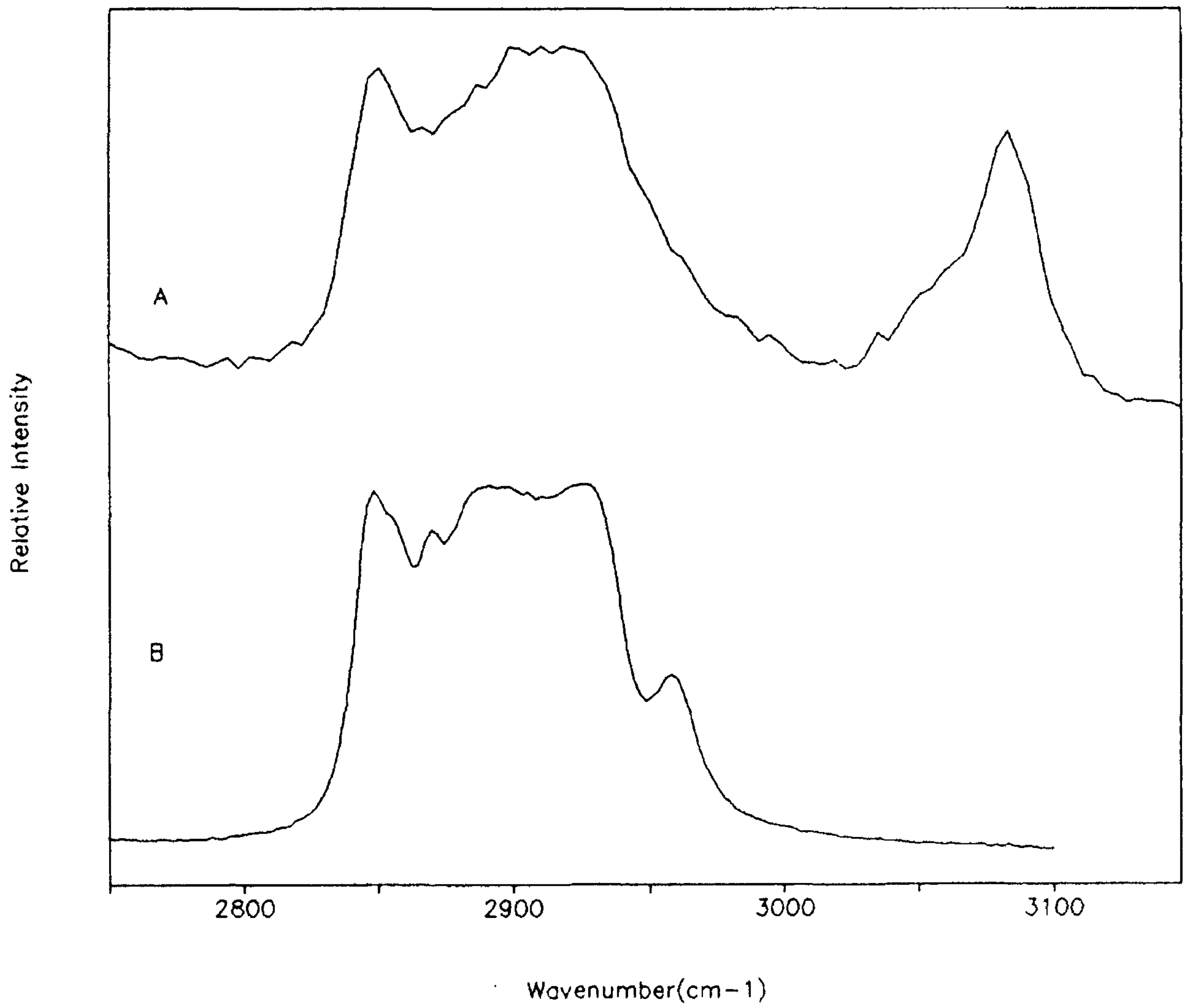
A
B
Relative Intensity
2800
2900
3000
3100
Wavenumber(cm-1)

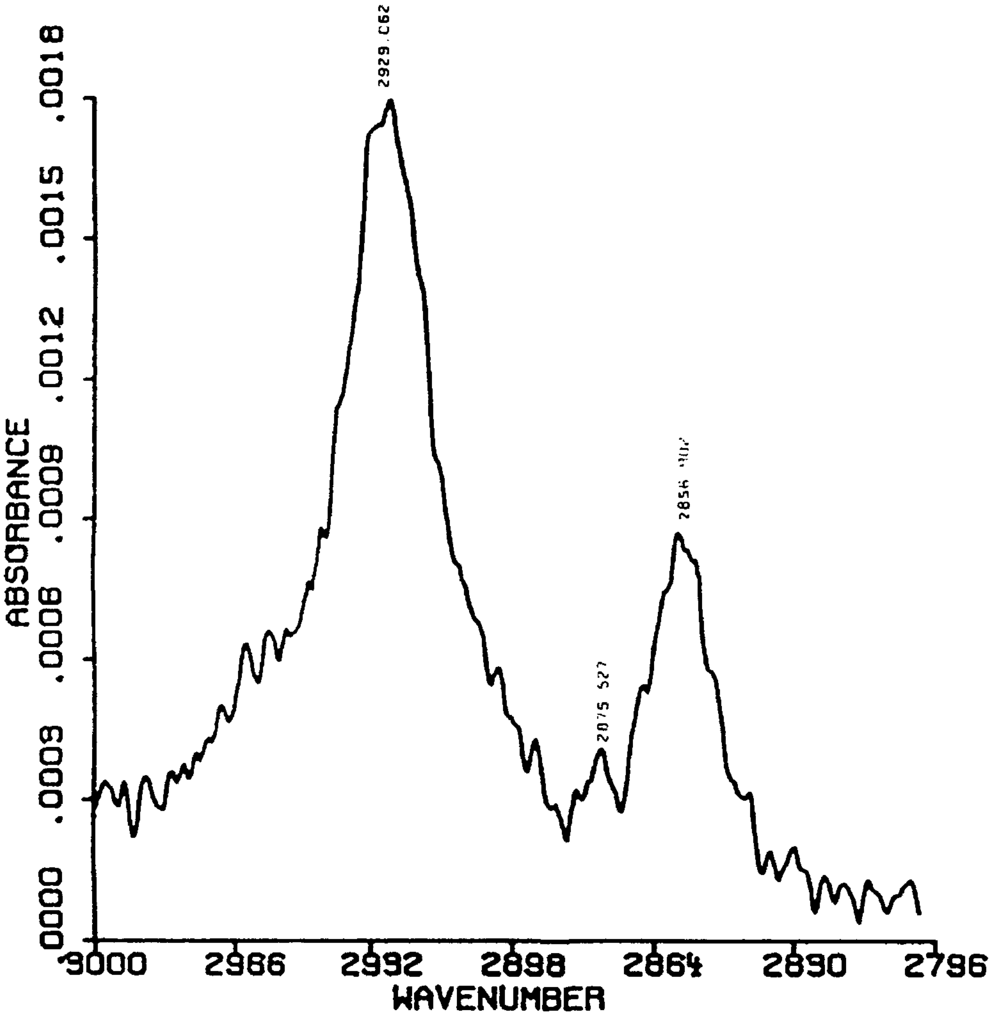
2929.062
2875.527
2856
ABSORBANCE
.0000
.0003
.0006
.0009
.0012
.0015
.0018
3000
2966
2932
2898
2864
2830
2796
WAVENUMBER

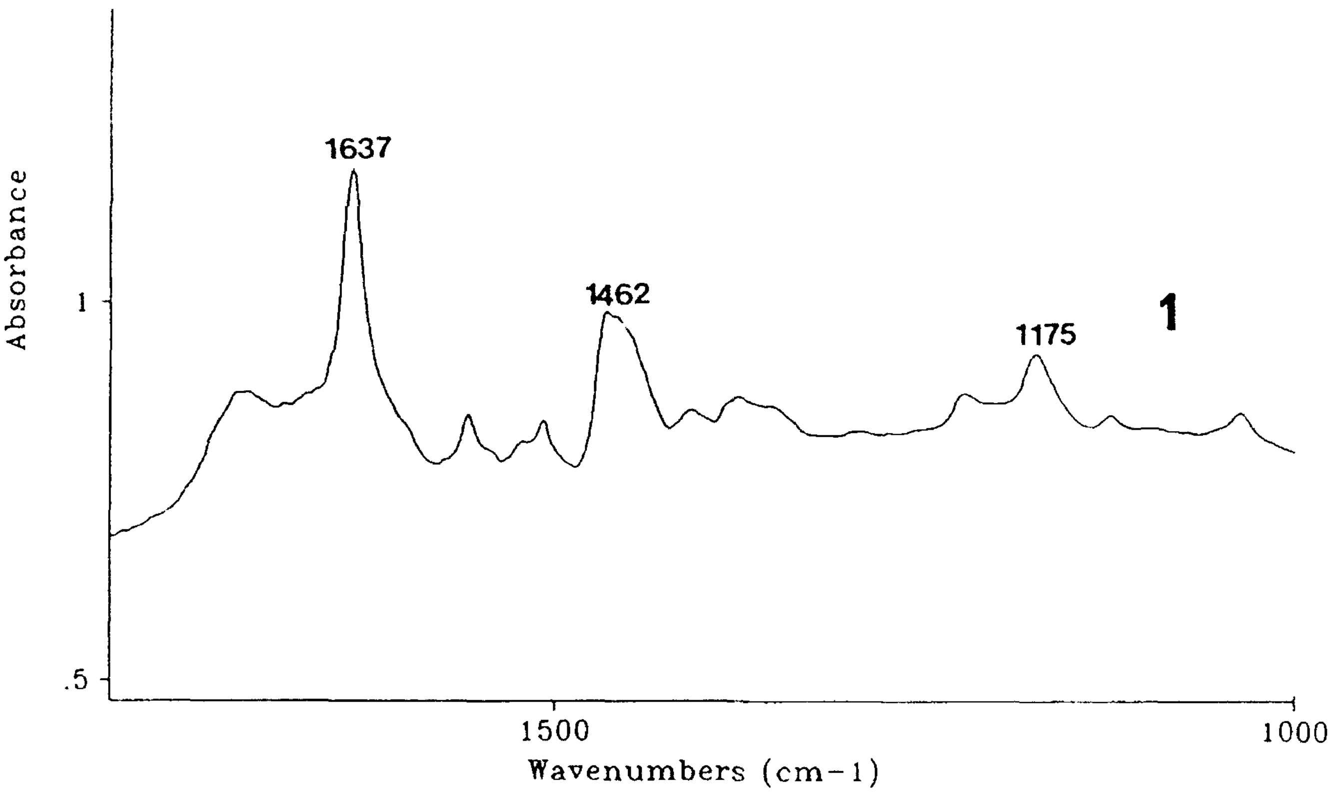
1637
1462
1175
1
Absorbance
1
.5
1500
1000
Wavenumbers (cm-1)

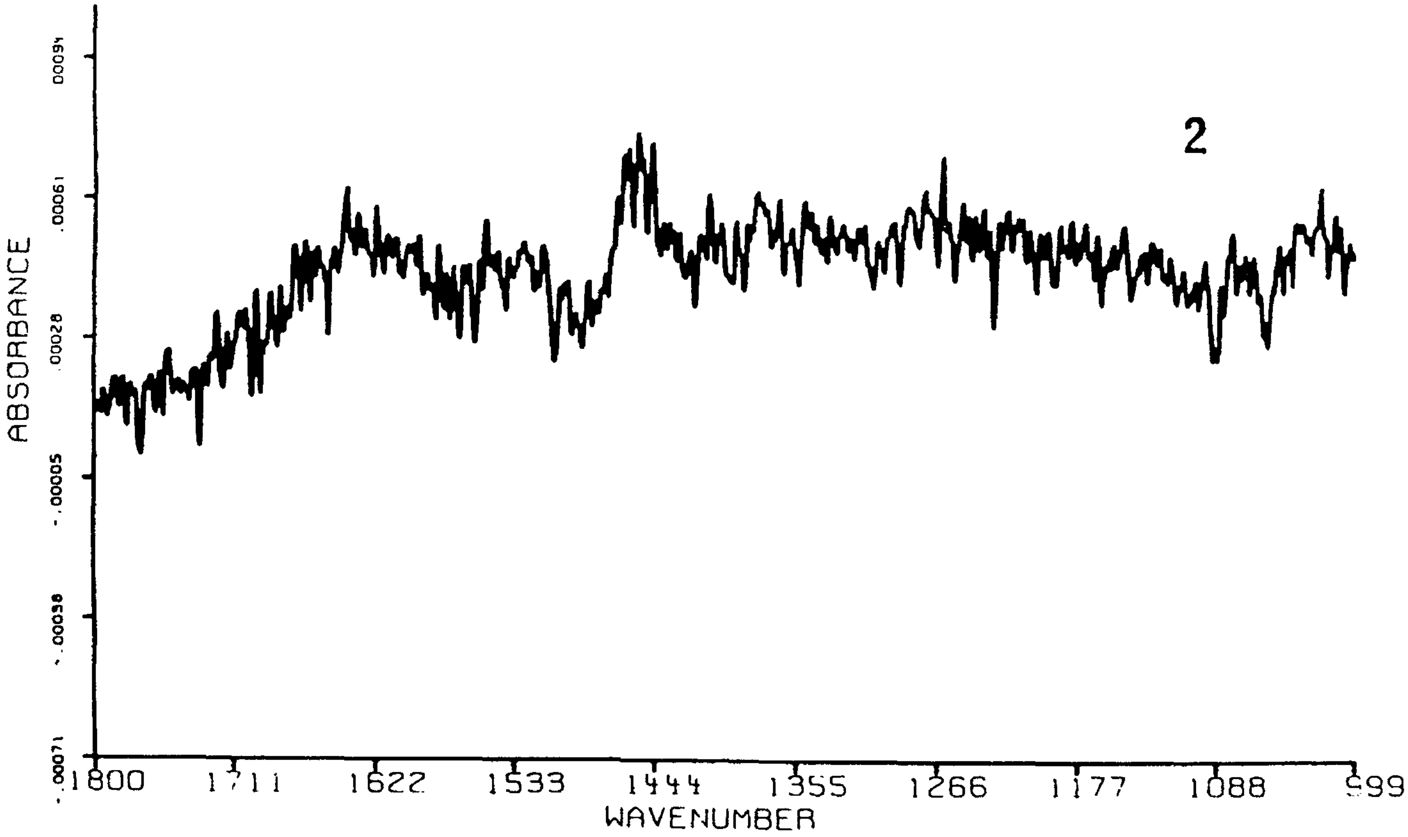
2
ABSORBANCE
.00094
.00061
.00028
-.00005
-.00038
-.00071
1800
1711
1622
1533
1444
1355
1266
1177
1088
999
WAVENUMBER

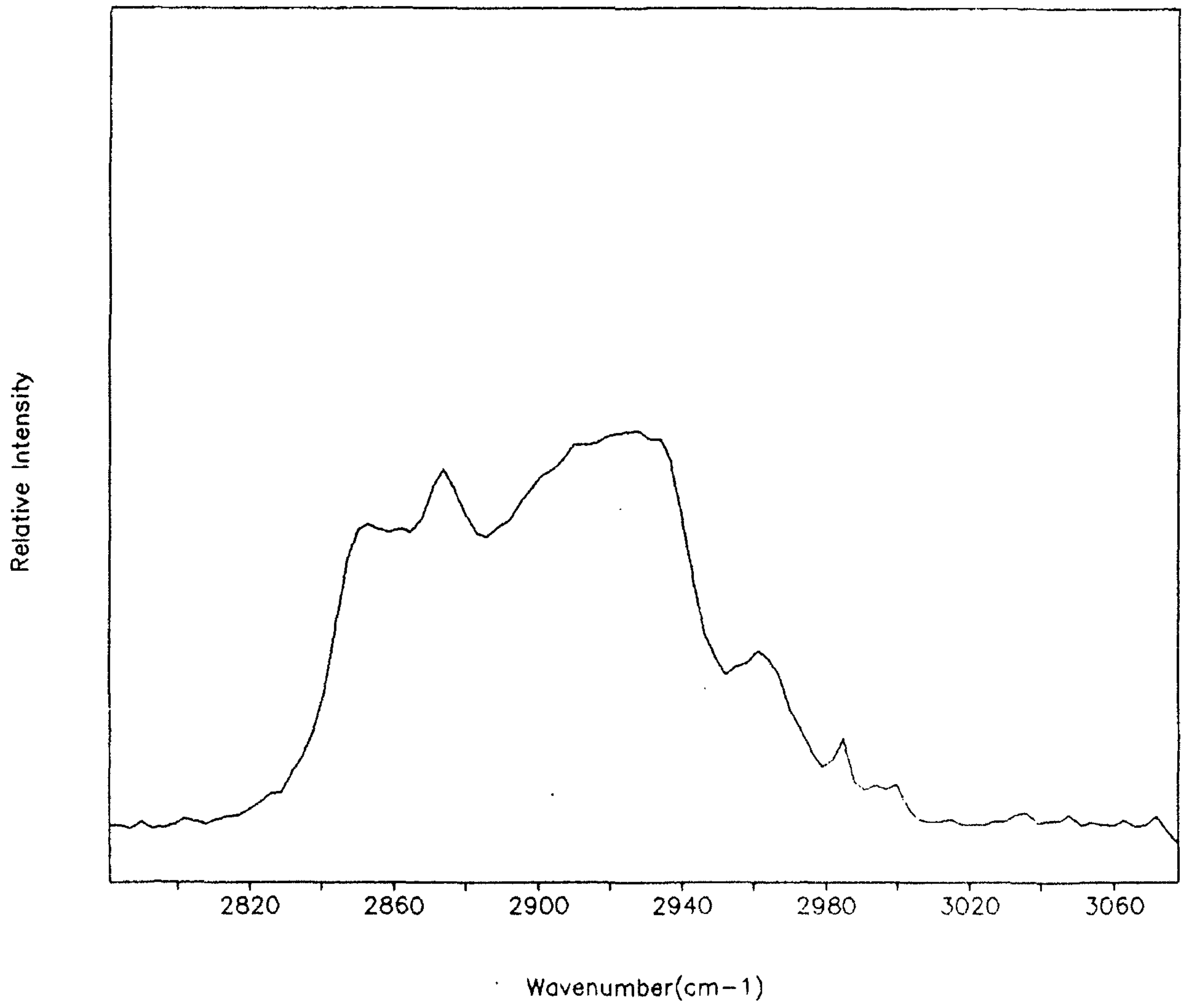
Relative Intensity
2820
2860
2900
2940
2980
3020
3060
Wavenumber(cm−1)

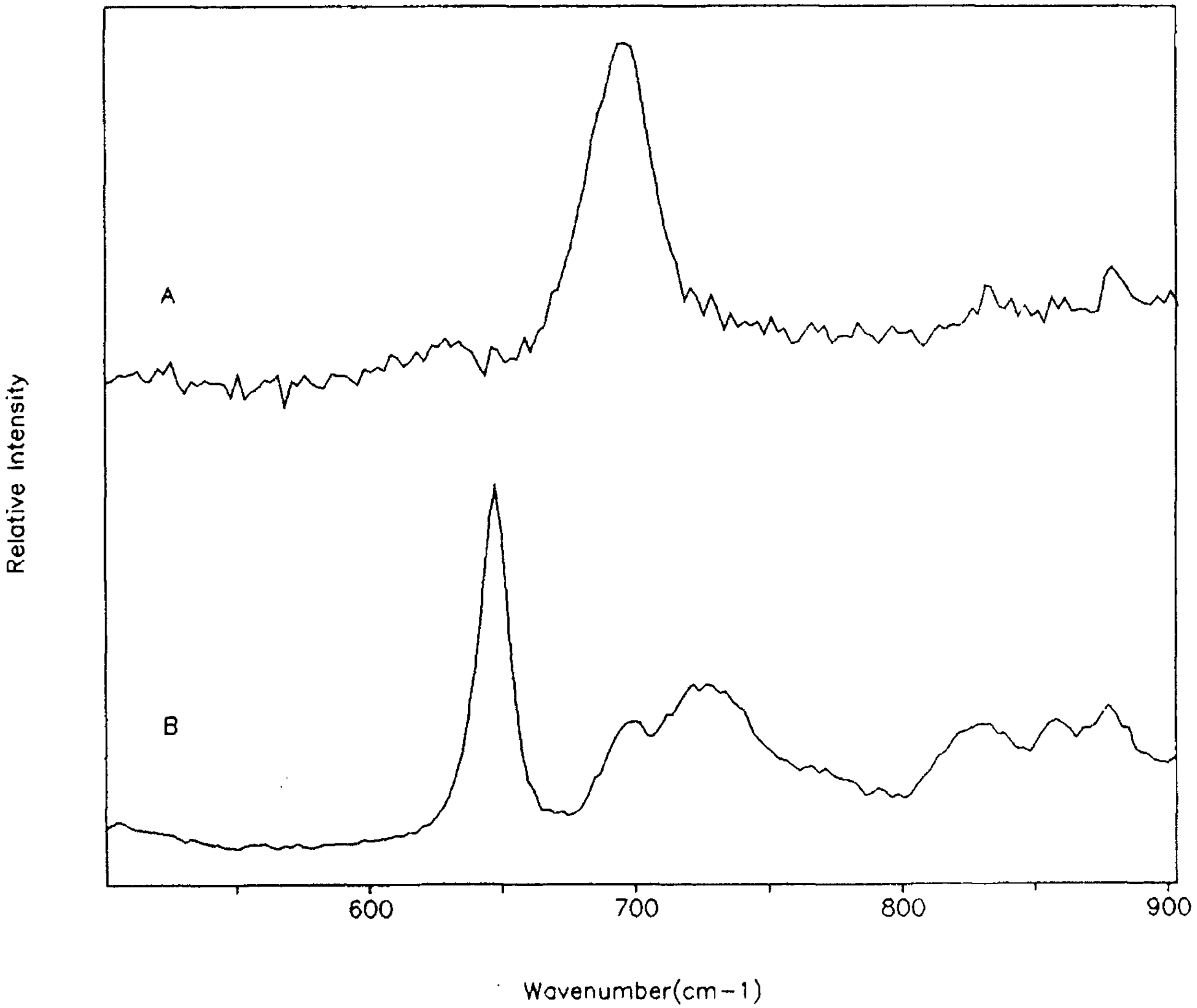
A
B
Relative Intensity
600
700
800
900
Wavenumber(cm−1)

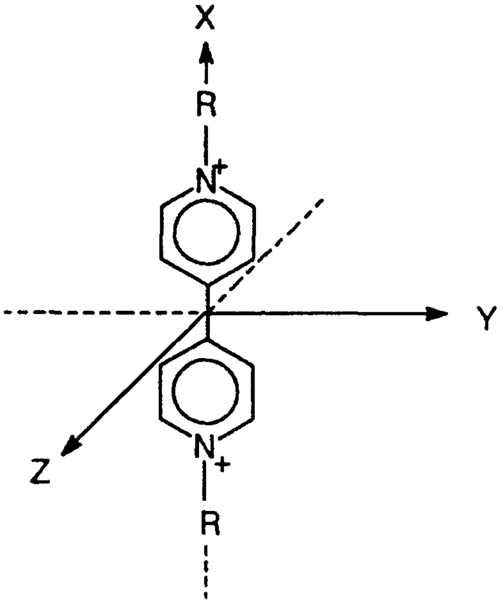
X
R
N+
Y
Z
N+
R